

## Linear and nonlinear optical properties of plasma-enhanced chemical-vapour deposition grown silicon nanocrystals

G. VIJAYA PRAKASH†, M. CAZZANELLI†, Z. GABURRO†,  
L. PAVESI†, F. IACONA‡, G. FRANZÒ§ and F. PRIOLO§

† INFN and Dipartimento di Fisica, Università di Trento, via  
Sommarive 14, 38050, Povo, Trento, Italy

‡ CNR-IMETEM, Stradale Primosole 50, 95121, Catania, Italy

§ INFN and Dipartimento di Fisica, Università di Catania, Corso Italia  
57, 95129 Catania, Italy

(Received 4 September 2001)

**Abstract.** We provide a systematic study on the linear and nonlinear optical properties of silicon nanocrystals (Si-nc) grown by plasma-enhanced chemical vapour deposition (PECVD). Linear optical properties, namely absorption, emission and refractive indices are reported. The sign and magnitude of both real and imaginary parts of third-order nonlinear susceptibility  $\chi^{(3)}$  of Si-nc are measured by the *Z*-scan method. Closed aperture *Z*-scan reveals a positive nonlinearity for all the samples. From the open aperture measurements, nonlinear absorption coefficients are evaluated and attributed to two-photon absorption. Absolute values of  $\chi^{(3)}$  are in the order of  $10^{-9}$  esu and show systematic correlation with the Si-nc size, due to quantum confinement related effects. A correlation has been made between  $\chi^{(3)}$ , nanocrystalline size, linear refractive index and optical band gap.

### 1. Introduction

In recent years, there has been considerable interest in semiconductor nanocrystals, because of their novel optical or physical properties which can be conveniently tailored over a broad range simply by altering their size [1]. Keeping in mind the technological importance of silicon, great interest was driven toward the Si nanostructures and, as a result, the observation of strong visible emission from porous Si provided great excitement [2]. However, owing to the poor photostability and uncertainty in the size of nanostructures in porous Si [3], the quest for controlled production of new materials based on silicon nanocrystals (Si-nc) is still going on. In a recent paper, we proposed preparation of Si-nc by plasma-enhanced chemical vapour deposition (PECVD) followed by high temperature annealing as a well-controlled system [4]. Optical and structural properties of these Si-nc have been investigated in [5].

A great impulse for Si-nc research is the recent observation of optical gain [6]. However, for photonic device applications such as all-optical switching, nonlinear optical properties are of major interest. Intensity-dependent changes in the optical properties are prominent at high intensities (*I*) of a pump laser, particularly third-order nonlinear effects. This third-order nonlinearity can be described by

nonlinear refraction ( $\gamma$ ) and nonlinear absorption ( $\beta$ ) parameters. They are related at high intensities to the refractive index and absorption coefficients, respectively, by  $n(I) = n_0 + \gamma I$  and  $\alpha(I) = \alpha_0 + \beta I$ , where  $n_0$  and  $\alpha_0$  stand for linear refractive index and linear absorption coefficient [7]. The nonlinear parameters  $\gamma$  and  $\beta$  are related to the real and imaginary parts of third-order nonlinear susceptibilities ( $\chi^{(3)}$ ).

Until now, nonlinear optical properties have been studied on Si-nc prepared by sol-gel, laser ablation and ion implantation or on porous Si [8–11]. However, the role of quantum confinement and interface states in the nonlinear properties of Si-nc has not been clarified yet. The differences in sample characteristics and fabrication methods can account for the large variation in observed nonlinear optical coefficients.

In this article, we present a detailed report on the linear and nonlinear optical properties of PECVD grown Si-nc. The dimensions of the Si-nc are well controlled by the excess Si content as well as temperature of annealing at the growing level. The absorption, emission and linear refractive indices for different Si-nc are reported. The sign and magnitude of both real and imaginary parts of third-order nonlinear susceptibilities,  $\chi^{(3)}$ , for different sized Si-nc are measured by the Z-scan method. A specific correlation is made between the nanocrystal size,  $\chi^{(3)}$ , linear refractive index and optical band gap.

## 2. Experimental set-up

Stoichiometric  $\text{SiO}_x$  films were prepared by using a parallel plate PECVD system followed by high temperature annealing [4]. These films were deposited on a quartz substrate in a three-layer waveguide geometry. Two 100 nm thick  $\text{SiO}_2$  films sandwiched a 230 nm thick  $\text{SiO}_x$  layer. An error of  $\pm 30$  nm can be estimated for the thickness of the films. High temperature annealing of  $\text{SiO}_x$  films leads to the separation of the  $\text{SiO}_x$  in Si and  $\text{SiO}_2$ . As a consequence, Si-nc embedded in a  $\text{SiO}_2$  matrix are formed [4]. The size of Si-nc increases with increasing excess of Si, as well as with increasing annealing temperature (table 1). The formation of Si-nc and their sizes were confirmed by transmission electron microscopy (TEM) analysis. A detailed preparation procedure could be found in our earlier works [4, 5]. It was noted from Rutherford backscattering (RBS) measurements, that, with our deposition technique, nitrogen incorporation in the film occurs [4].

We performed Z-scan experiments on Si-nc by using a Gaussian laser beam (Ti:sapphire laser, wavelength  $\lambda = 813$  nm with a repetition rate of 82 MHz and with 60 fs pulse width) in a tight focus limiting geometry (figure 1). The beam waist at the focus of the lens was typically  $19 \mu\text{m}$  with peak intensity ( $I_0$ ) up to  $2 \times 10^{10} \text{ W cm}^{-2}$ .  $I_0$  was varied by using neutral density filters. While a computer-driven continuous motor moves the sample along the optical path ( $z$  axis), the transmission through the sample is monitored by a silicon photodiode (D1). An aperture is placed in front of D1 for closed aperture measurements. A small portion of the input intensity was monitored by another photodiode (D2) and the ratio (D1/D2) is recorded as a function of the sample position,  $z$ . Transmission with and without the aperture was measured in the far field as the sample moved through the focal point, enabling the separation of the nonlinear refractive index from the nonlinear absorption. The experimental set-up was checked by measuring a reference sample  $\text{CS}_2$  [12].

Table 1. Total Si content (obtained from RBS measurements), temperatures of thermal treatment, Si-nc radius estimated from TEM measurements, optical band gap ( $E_{g2}$ ), PL maxima ( $E_m$ ), linear refractive index ( $n$ ), absorption coefficients at 400 nm ( $\alpha_0$ ), nonlinear absorption coefficients ( $\beta$ ), real ( $\text{Re}\chi^{(3)}$ ) and imaginary ( $\text{Im}\chi^{(3)}$ ) parts of third-order nonlinear susceptibilities and absolute third-order nonlinear susceptibilities ( $\chi^{(3)}$ ).

Sample name	Si content (at.%)	Annealing temperature ( $^{\circ}\text{C}$ )	Si-nc radius (nm)	Optical				Refractive index	$\alpha_0^a$ ( $\times 10^3 \text{ cm}^{-1}$ )	$\beta$ ( $\text{m GW}^{-1}$ )	$\text{Re}\chi^{(3)}$ ( $10^{-9} \text{ esu}$ )	$\text{Im}\chi^{(3)}$ ( $10^{-10} \text{ esu}$ )	$\chi^{(3)}$ ( $10^{-9} \text{ esu}$ )
				band gap <sup>a</sup> (eV)	Emission maxima <sup>a</sup> (eV)	Emission band gap <sup>a</sup> (eV)	Si-nc radius (nm)						
1C	46	1100	1.0	$2.75 \pm 0.05$	1.34	2.15	16.3	$1.4 \pm 0.3$	$1.46 \pm 0.5$	$2.1 \pm 0.4$	$1.4 \pm 0.5$		
3C	42	1100	$\leq 0.7$	$3.30 \pm 0.05$	1.45	1.84	9.9	$0.16 \pm 0.03$	$0.96 \pm 0.2$	$0.28 \pm 0.03$	$0.9 \pm 0.2$		
5C	39	1100	$< 0.7$	$3.38 \pm 0.05$	1.69	1.93	3.2	$0.2 \pm 0.03$	$2.7 \pm 0.5$	$0.3 \pm 0.04$	$2.7 \pm 0.5$		
1B	46	1200	1.3	$2.98 \pm 0.05$	1.33	2.03	13.8	$0.09 \pm 0.04$	$0.33 \pm 0.01$	$0.11 \pm 0.08$	$0.33 \pm 0.01$		
3B	42	1200	0.7	$3.41 \pm 0.05$	1.42	1.84	10.0	$0.15 \pm 0.06$	$0.39 \pm 0.06$	$0.23 \pm 0.02$	$0.39 \pm 0.06$		
5B	39	1200	$< 0.7$	$3.52 \pm 0.05$	1.58	1.66	4.1	$1.59 \pm 0.02$	$0.79 \pm 0.03$	$2.3 \pm 0.4$	$0.79 \pm 0.03$		
1A	46	1250	2.1	$3.04 \pm 0.05$	1.33	2.00	12.7	-	$0.42 \pm 0.02$	-	$0.42 \pm 0.02$		
3A	42	1250	1.7	$3.45 \pm 0.05$	1.36	1.82	9.1	-	$0.62 \pm 0.02$	-	$0.62 \pm 0.02$		
5A	39	1250	1.5	$3.63 \pm 0.05$	1.56	1.66	4.1	$0.4 \pm 0.07$	$1.3 \pm 0.2$	$0.6 \pm 0.1$	$1.3 \pm 0.2$		

<sup>a</sup> From [5].

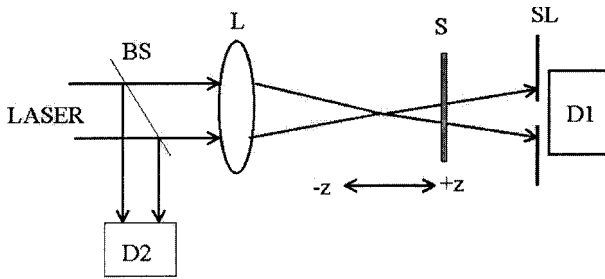


Figure 1. Z-scan set-up. D1 and D2 are silicon photodiodes, BS is a beam splitter, L is the lens, S is the sample and SL is a variable slit.

Absorption spectra were measured using a UNICAM UV-visible spectrometer with quartz as reference. The photoluminescence (PL) was measured by exciting the sample with the 488 nm line of an Ar-ion laser with power 10 mW. The emission was collected through a monochromator which is coupled to a photomultiplier tube or a liquid nitrogen cooled Ge detector. As the sample structure was a waveguide, the linear refractive indices for these samples were measured using a prism coupling (*m*-line) technique with the 633 nm line of a He-Ne laser [13]. We found one weakly guiding mode for all the samples under investigation. The observed guided mode in TE and TM polarizations are used to estimate the linear refractive index and thickness of the samples. The refractive indices are given in table 1, while the estimated thicknesses were consistent with the growth parameters.

### 3. Results and discussion

Room temperature absorption and photoluminescence (PL) spectra of various Si-nc embedded SiO<sub>2</sub> samples are reported in figure 2. With the decrease of both Si content as well as annealing temperature, the PL peak maxima shift to blue. From the sharp rising edge of the absorption spectra the optical band gap values can be evaluated [5]. In a similar way to PL, the optical band gaps ( $E_{g2}$ ) also show a progressive blue shift with decreasing Si content and annealing temperatures. These results were attributed to quantum confinement related effects and to the active role of radiative interface states [5].

Linear refractive indices (*n*) for different Si-nc are obtained from the *m*-line measurements (table 1). As our samples are a mixture of Si-nc and SiO<sub>2</sub>, *n* values are expected to be lower than that of c-Si and to increase with Si content. Table 1 shows this general trend. We estimated the refractive index values for different Si contents in the films by using the Bruggemann effective medium approximation [14], assuming the Si-nc is embedded in the SiO<sub>2</sub> medium. The estimated values are systematically lower than those measured (table 2). However, RBS data show the presence of nitrogen in the SiO<sub>x</sub> films up to an atomic percentage of 10% [4]. Hence we repeated the calculation by assuming Si-nc in a medium composed by both SiO<sub>2</sub> and Si<sub>3</sub>N<sub>4</sub> (table 2). Despite the rather crude approximation of a complete phase separation between SiO<sub>2</sub> and Si<sub>3</sub>N<sub>4</sub>, good agreement is found for the samples annealed at the highest temperature. However, with this crude model, we cannot reproduce the annealing temperature dependence or the differences

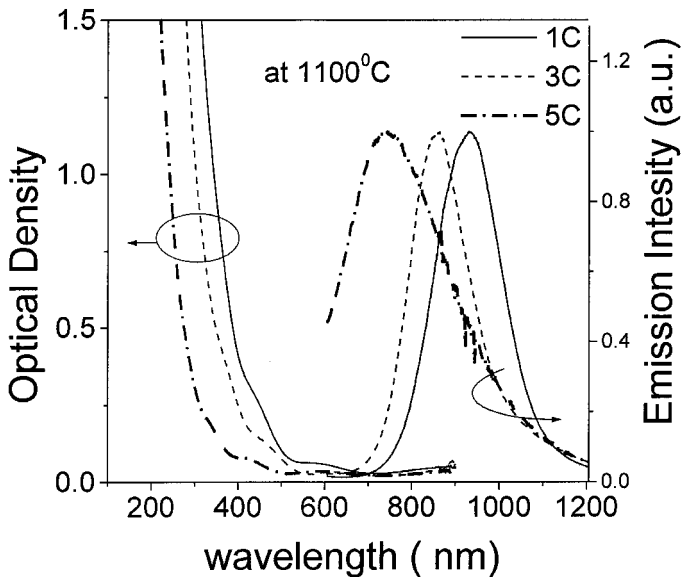


Figure 2. Absorption and emission spectra for different Si contents at 1100°C annealing temperature. The sample name refers to those given in table 1.

Table 2. Atomic contents of silicon (Si), oxygen (O) and nitrogen (N) (from RBS measurements), measured refractive index at 1250°C annealing temperature and estimated refractive indices from the Bruggemann approximation (assuming Si-nc in SiO<sub>2</sub> medium or Si-nc in SiO<sub>2</sub>-Si<sub>3</sub>N<sub>4</sub> medium).

Atomic Si content (Si at.%)	Atomic O content (O at.%)	Atomic N content (N at.%)	Measured refractive index at 1250°C annealing	Refractive index from Bruggemann approximation	
				Si-SiO <sub>2</sub>	Si-SiO <sub>2</sub> -Si <sub>3</sub> N <sub>4</sub>
46	45	9	2.00	1.91	2.00
42	48	10	1.82	1.75	1.80
39	49	12	1.66	1.64	1.66

measured in different sets. These estimations rather suggest that the presence of N in the film does influence the optical properties of the Si-nc through the formation of a composite matrix. A more sophisticated theory for the refractive index is needed to clarify all these aspects.

Z-scan experiments were performed to measure the third-order nonlinear coefficients. Representative data for sample 3A are given in figure 3. The normalized transmission for a closed aperture scan (finite aperture at the far field) is given by [9, 12]

$$T(z) = 1 + \frac{4x\Delta\phi}{(x^2 + 9)(x^2 + 1)}, \quad (1)$$

where  $\Delta\phi$  is the nonlinear phase change,  $x = z/z_0$ , and  $z_0$  is the Rayleigh range of the lens given by  $z_0 = \pi w_0^2/\lambda$ .  $w_0$  is the beam waist at the focus and  $\lambda$  is the

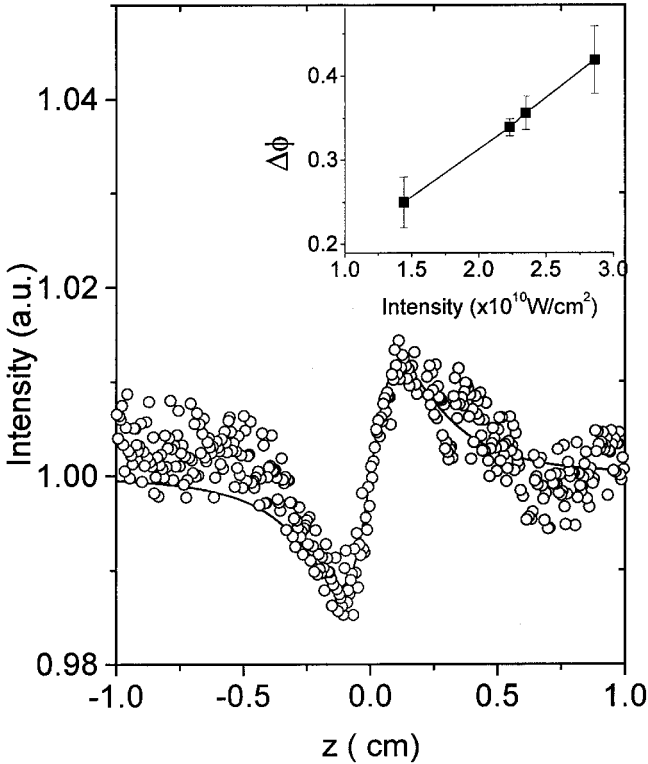


Figure 3. Closed aperture Z-scan for sample 3A at intensity  $2.9 \times 10^{10} \text{ W cm}^{-2}$ . The solid line is the theoretical fit with equation (1). Inset shows the variation of  $\Delta\phi$  with the incident intensity.

wavelength of the laser. The measured data are fitted by equation (1) to obtain  $\Delta\phi$  values. It is also possible to estimate  $\Delta\phi$  by measuring the peak-to-valley variations from the  $z$  scan trace ( $\Delta T_{p-v}$ ) [12]

$$\Delta T_{p-v} \cong 0.406(1 - S)^{0.25} |\Delta\phi|, \quad (2)$$

where  $S$  is the aperture linear transmittance given as  $1 - \exp(2r_a^2/w_a^2)$ .  $r_a$  and  $w_a$  stands for aperture radius and beam radius at the aperture, respectively. Both these estimations are used and give the same values for  $\Delta\phi$ . The nonlinear index of refraction ( $\gamma$ ) is related to  $\Delta\phi$  by

$$\gamma = \frac{\Delta\phi\lambda\alpha}{2\pi I_0[1 - \exp(-\alpha l)]}, \quad (3)$$

where  $\alpha$  is the measured absorption coefficient at 813 nm,  $l$  is the SiO<sub>x</sub> layer thickness and  $I_0$  is the peak intensity at the focus. Let us note that  $\gamma$  does not depend on the precise value of  $\alpha$  used since  $\alpha l \ll 1$  (figure 2).

The experiments were also performed on the pure quartz substrate and no significant contribution from the quartz substrate was found. The signature of the closed aperture data for all the samples is a distinct valley–peak configuration suggesting a positive nonlinear effect (self-focusing), as expected for most of the dispersive materials [8, 9, 13]. We found a linear dependence of  $\Delta\phi$  on  $I_0$  and the

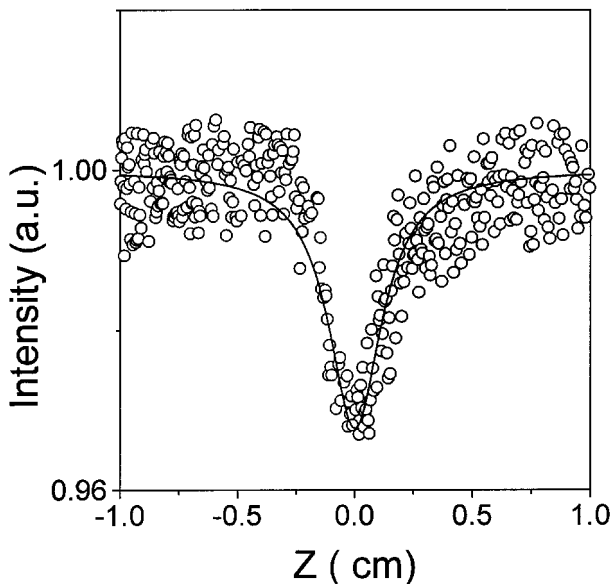


Figure 4. Open aperture  $Z$ -scan for sample 5B at intensity  $1.7 \times 10^{10} \text{ W cm}^{-2}$ . The solid line is the theoretical fit using equation (4).

corresponding  $\gamma$  values are substituted in the equation,  $\text{Re } \chi^{(3)} = 2n^2 \varepsilon_0 c \gamma$ , to obtain the real part of the third-order nonlinear susceptibilities (table 1), where  $\varepsilon_0$  is the permittivity of free space and  $c$  is the velocity of light.

It was reported that the use of high repetition rate lasers may give rise to thermal optical nonlinearity due to acoustic effects and induced cumulative heating effects, especially in liquids and in some optical glassy materials [15–17]. In order to give a crude estimation of the thermal contributions we used the model of [12] with the Si parameters, i.e. thermal refractive index changes  $dn/dT = 2.4 \times 10^{-4} \text{ K}^{-1}$  at 1024 nm [18], specific heat  $0.72 \text{ J g}^{-1} \text{ K}^2$  and density  $2.33 \text{ g cm}^{-2}$  [8, 19]. At the maximum power of the pump laser, the thermal contribution to  $\text{Re } \chi^{(3)}$  is in the order of  $10^{-13}$  esu. This value is almost four orders of magnitude lower than the measured values. Even during a 3-h long experiment, we do not observe any changes in the  $Z$ -scan trace. Moreover, we also conducted closed  $Z$ -scan experiments by chopping the laser (down to 100 Hz) to avoid cumulative heating effects within the sample [15]. While for a liquid sample  $\text{CS}_2$ , which is prone to give thermal induced effects [16] we do observe a decrease in the  $\Delta T_{p-v}$  values with increasing chopper frequency; for Si-nc samples we do not observe any changes. Hence, the thermal contributions are negligible and the optical nonlinearities are mainly refractive.

Figure 4 shows the normalized open aperture transmission (full power into the detector) as a function of  $z$ . A symmetric bell-shaped transmission is measured with minimum at the focus ( $z = 0$ ). One can deduce the nonlinear absorption coefficient,  $\beta$ , from the open aperture  $Z$ -scan data from the equation [9]

$$T(z) = 1 + \frac{\beta I_0 l}{\left(1 + \frac{z^2}{z_0^2}\right)}. \quad (4)$$

The open aperture experiment is performed repeatedly and for different peak intensities between  $0.3$  to  $2 \times 10^{10} \text{ W cm}^{-2}$  to ensure proper measurements. The  $\beta$  values are used to evaluate the imaginary part of the third-order nonlinear susceptibility  $\chi^{(3)}$  by  $\text{Im} \chi^{(3)} = n^2 \varepsilon_0 c \lambda \beta / 2\pi$ . Results are reported in table 1. On comparison, the measured  $\beta$  values for Si-nc are higher than the value for crystalline silicon (c-Si) [20, 21] and close to the values quoted for porous silicon [8].

The nonlinear absorption in most of the refractive materials arises from either direct multiphoton absorption or saturation of single photon absorption [12]. It is interesting to note that the nonlinear absorption in silicon nanocrystals formed by ion implantation and laser ablation depends on the excitation energy as well as Si-nc size [9, 10, 22, 27]. For example, laser ablated samples exhibit saturation of absorption and bleaching effects: change of sign for nonlinear absorption from positive to negative with the increase of pump intensity at the near resonant excitations (355 and 532 nm) [23]. By contrast, ion implanted samples show an almost linear dependence of  $\beta$  with the pump power, clear evidence of two-photon nonlinear processes [22]. In our case, we found a well-defined bell-shaped minimum transmittance at  $z = 0$  for all the laser intensities used. In addition, the laser energy ( $\hbar\omega$ ) used is such that  $E_{g2} < 2\hbar\omega < 2E_{g2}$ . Both these features suggest two-photon absorption (TPA) as the origin of the nonlinear absorption. Finally, the absorption at 813 nm is extremely weak or even negligible (figure 2). Similar conclusions were obtained for p-Si [8]. The present  $\beta$  values are enhanced by two orders of magnitude than the theoretically predicted TPA coefficient for c-Si, probably due to quantum confinement related effects [24]. The highest TPA coefficient is observed for sample 5B while the lowest is for 1B. For large Si-nanocrystal containing samples (1A and 3A) we were not able to observe any significant TPA traces.

The absolute values for  $\chi^{(3)}$  are calculated from  $[(\text{Re} \chi^{(3)})^2 + (\text{Im} \chi^{(3)})^2]^{1/2}$ . By comparing  $\text{Re} \chi^{(3)}$  and  $\text{Im} \chi^{(3)}$  one can conclude that  $\text{Re} \chi^{(3)} \gg \text{Im} \chi^{(3)}$ , that is the nonlinearity is dominantly refractive. The absolute values for  $\chi^{(3)}$  are of the same order of magnitude as those reported for porous silicon [8], for glasses containing microcrystallites [25] and close to those expected theoretically for low-dimensional Si materials ( $\chi^{(3)} \sim 10^{-8}$  esu) [26, 27]. Figure 5 shows the variation with different Si contents and annealing temperatures. Similar to the observations made by PL, the third-order nonlinear susceptibility values show systematic variation with respect to Si-nc size. As for the temperature dependence, the  $1200^\circ\text{C}$  annealed samples show the lowest  $\chi^{(3)}$  values for all the Si content. At present we cannot see the reason for this.

Figure 6 shows an increasing trend of  $\chi^{(3)}$  with respect to Si-nc radius ( $r$ ). The inset on the figure reports the PL maxima ( $E_m$ ) variation with Si-nc radii. Both data can be fitted by a dependence of  $1/r^{1.39}$ . For  $E_m$  this is an expected trend for quantum confinement related effects [28]. Hence the present study suggests that large third-order nonlinear coefficients observed for small nanocrystals are due to an increased quantum confinement effect. A direct comparison of  $\chi^{(3)}$  values measured here with those for the Si-nc prepared by other methods is difficult because of the significant variation in the preparation method, Si-nc size, wavelength of the pump laser and pump power [11, 22, 23].

On the other hand, it is of particular interest to obtain a relation between  $\chi^{(3)}$  and other optical properties. Attempts were made for a large number of refractive

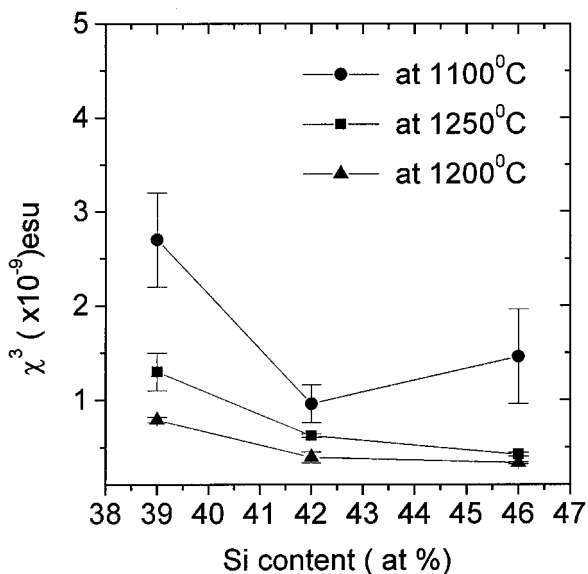


Figure 5.  $\chi^{(3)}$  for different Si content at different annealing temperatures.

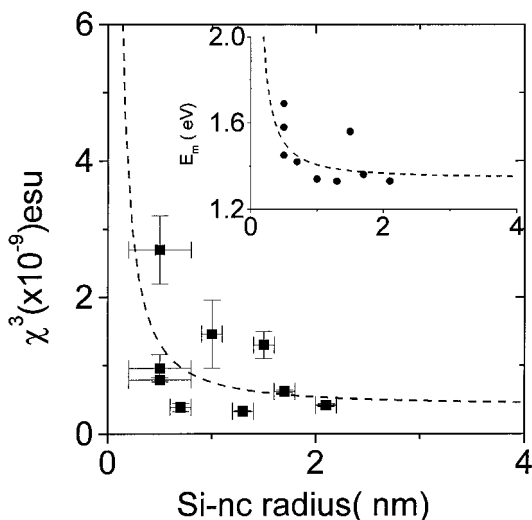


Figure 6. Variation of  $\chi^{(3)}$  with Si-nc radius ( $r$ ). The error bars on the radius refer to the width of the size histogram measured by TEM. Inset shows the PL peak maxima variation with Si-nc radius. Dashed lines are  $1/r^{1.39}$  dependence fits.

materials to obtain a relation between polarizability, linear and nonlinear refractive indices and optical band gap [29–33]. It was empirically established that  $\chi^{(3)}$  relates to the optical band gap in most inorganic materials [30]. Similarly, the effective polarizability, which is proportional to  $1 - [(n^2 - 1)/(n^2 + 2)]$ , also shows a linear relation with the square root of the optical band gap with a slope of 1.23 for numerous optical materials [29, 31–33]. A plot of  $\chi^{(3)}$  with respect to the effective polarizability and ( $E_{g2}^{1/2}$ ) is presented in figure 7.  $\chi^{(3)}$  increases with increasing

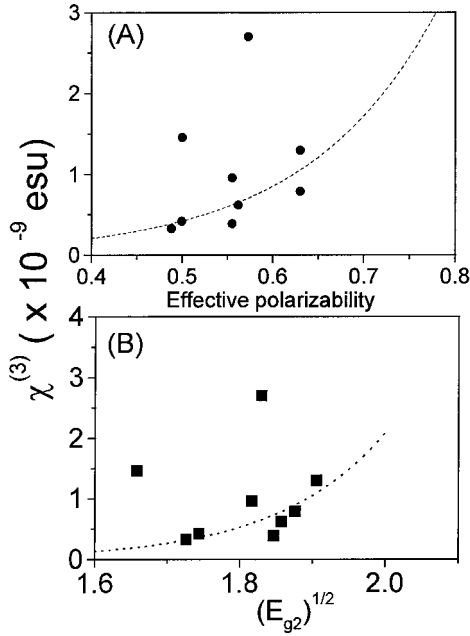


Figure 7. Variation of  $\chi^{(3)}$  with (a) effective polarizability,  $1 - [(n^2 - 1)/(n^2 + 2)]$ , and (b) optical band gap. The dotted lines are to guide the eye.

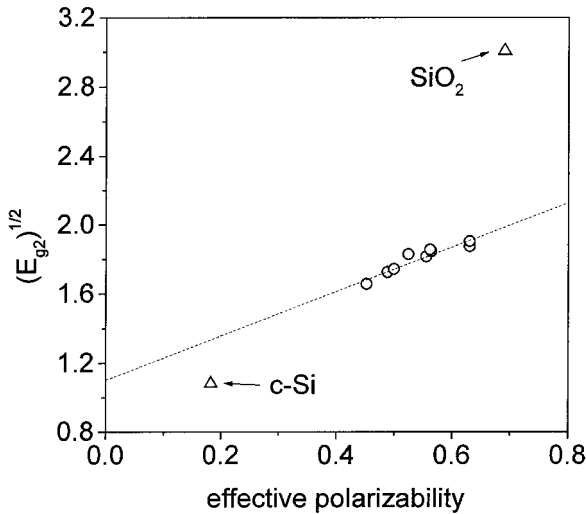


Figure 8. Variation of effective polarizability,  $1 - [(n^2 - 1)/(n^2 + 2)]$ , with optical band gap  $(E_{g2}^{1/2})$  for Si-nc. The data for c-Si and for  $\text{SiO}_2$  are also shown as open triangles ( $\Delta$ ).

effective polarizability as well as optical band gap. Some data points do not clearly illustrate this, but an overall trend is clear. Figure 8 shows the linear increase of  $E_{g2}^{1/2}$  with the effective polarizability, the slope is 1.42, i.e. close to the observations made for other optical materials [29–33]. It is thus shown that  $\chi^{(3)}$ ,  $E_{g2}$  and  $n$  are correlated within the experimental scatters of the data. Smaller nanocrystals possess larger  $\chi^{(3)}$  and optical band gaps with lower refractive index.

#### 4. Conclusions

Si-nc formed by high temperature annealed PECVD deposited SiO<sub>x</sub> films have been characterized for linear and nonlinear properties. The third-order nonlinear coefficients have positive sign and the values are two orders of magnitude higher than bulk silicon. The dependence of  $\chi^{(3)}$  with respect to the Si-nc size is mainly related to quantum confinement effects, similar to the PL and absorption measurements. The nonlinear absorption observed is ascribed to two-photon absorption. About two orders of magnitude higher values of the real part of  $\chi^{(3)}$  than the imaginary part of  $\chi^{(3)}$  indicate that the observed nonlinearities are dominantly refractive.

#### Acknowledgments

This work has been supported by MURST through project COFIN99 (MODESTI) and by INFN through the project RAMSES. We thank Dr M. Ferrari and his group for lending us the *m*-line measurement facility.

#### References

- [1] NALWA, H. S., 2000, *Hand Book of Nanostructured Materials and Nanotechnology*, Vol. 4 (CA: Academic Press).
- [2] CANHAM, L. T., 1990, *Appl. Phys. Lett.*, **57**, 1046.
- [3] BISI, O., OSSICINI, S., and PAVESI, L., 2000, *Surf. Sci. Rep.*, **38**, 1.
- [4] IACONA, F., FRANZÒ, G., and SPINELLA, C., 2000, *J. appl. Phys.*, **87**, 1295.
- [5] VIJAYA PRAKASH, G., DALDOSSO, N., DEGOLI, E., IACONA, F., PUCKER, G., CAZZANELLI, M., ROCCA, F., GABURRO, Z., DALBA, P., CERETTA MOREIRA, E., PACICI, D., FRANZÒ, G., PRIOLO, F., ARCANGELI, C., FILONOV, A. B., OSSICINI, S., and PAVESI, L., 2001, *J. Nano Sci. Nano Tech.*, **1**, 159.
- [6] PAVESI, L., DAL NEGRO, L., MAZZOLENI, C., FRANZÒ, G., and PRIOLO, F., 2000, *Nature*, **408**, 440.
- [7] SHEN, Y. R., 1984, *The Principle of Nonlinear Optics* (New York: Wiley).
- [8] HENARI, F. Z., MORGENSTERN, K., BLAU, W. J., KARAVANSKI, V. A., and DNEPROVSKII, V. S., 1995, *Appl. Phys. Lett.*, **67**, 323.
- [9] VIJAYA LAKSHMI, S., SHEN, F., and GREBEL, H., 1997, *Appl. Phys. Lett.*, **71**, 3332.
- [10] VIJAYA LAKSHMI, S., GEORGE, M. A., and GREBEL, H., 1997, *Appl. Phys. Lett.*, **70**, 708.
- [11] BORSELLA, E., FALCONIERI, M., BOTTI, S., MARTELLI, S., BIGNOLI, F., COSTA, L., GRANDI, S., SANGALETTI, L., ALLIERI, B., and DEPERO, L., 2001, *Mat. Sci. Eng. B*, **79**, 55.
- [12] SHEIK-BAHAË, M., SAID, A. A., and VAN STRYLAND, E. W., 1989, *Optics Lett.*, **14**, 955.
- [13] TOWNSEND, P. D., BAKER, G. L., SCHLOTTER, N. E., KLAUSNER, C. F., and ETEMAD, S., 1988, *Appl. Phys. Lett.*, **53**, 1782.
- [14] THEISS, W., 1997, *Surf. Sci. Rep.*, **29**, 91.
- [15] FALCONIERI, M., 1999, *J. Opt. A: Pure appl. Opt.*, **1**, 662.
- [16] FALONIERI, M., and SALVETTI, G., 1999, *Appl. Phys. B*, **69**, 133.
- [17] LI, H. P., KAM, C. H., LAM, Y. L., JIE, Y. X., JI, W., WEE, A. T. S., and HUAN, C. H. A., 2001, *Appl. Phys. B: Lasers Optics*, **72**, 611.
- [18] EICHELER, H. J., 1983, *Optics Commun.*, **45**, 62.
- [19] BERNINI, U., LETTIERI, S., MADDALENA, P., VITIELLO, R., and DI FRANCIA, G., 2001, *J. Phys: condens. Matter*, **13**, 1141.
- [20] REITZE, D. H., ZANG, T. R., WOOD, WM. M., and DOWNER, M. C., 1990, *J. opt. Soc. Am. B*, **7**, 84.
- [21] REINTJES, J. F., and MCGRODDY, J. C., 1973, *Phys. Rev. Lett.*, **30**, 901.
- [22] VIJAYALAKSHMI, S., GEBEL, H., YAGLIOGLU, G., PINO, R., DORSINVILLE, R., and WHITE, C. W., 2000, *J. appl. Phys.*, **88**, 6418.

- [23] VIJAYALAKSHMI, S., GEBEL, H., IQBAL, Z., and WHITE, C. W., 1998, *J. appl. Phys.*, **84**, 6502.
- [24] MURAYAMA, M., and NAKAYAMA, T., 1994, *Phys. Rev. B*, **49**, 5737; 1995, *Phys. Rev. B*, **52**, 4986.
- [25] VOGEL, E. M., WEBER, M. J., and KROL, D. M., 1991, *Phys. Chem. Glasses*, **32**, 231.
- [26] WANG, J., JIANG, H.-B., WANG, W.-C., ZHENG, J.-B., ZHANG, F.-L., HAO, P.-H., HOU, X.-Y., and WANG, X., 1992, *Phys. Rev. Lett.*, **69**, 3252.
- [27] CHEN, R., LIN, D. L., and MENDOZA, B., 1993, *Phys. Rev. B*, **48**, 11879.
- [28] LEDOUX, G., GUILLOIS, O., PORTERAT, D., REYNAUD, C., HUISKEN, F., KOHN, B., and PAILLARD, V., 2000, *Phys. Rev. B*, **62**, 15942.
- [29] DIMITROV, V., and SAKKA, S., 1996, *J. appl. Phys.*, **79**, 1736.
- [30] DIMITROV, V., and SAKKA, S., 1996, *J. appl. Phys.*, **79**, 1741.
- [31] DUEY, J. A., 1986, *J. solid state Chem.*, **62**, 145.
- [32] VITHAL, M., NACHIMUTHU, P., BANU, T., and JAGANNATHAN, R., 1997, *J. appl. Phys.*, **81**, 7922.
- [33] VIJAYA PRAKASH, G., 2000, *Mat. Lett.*, **46**, 15.